Chemistry–A European Journal
Research Article
doi.org/10.1002/chem.202302516
Chemistry Europe
European Chemical Societies Publishing
www.chemeurj.org

Hot Paper

Special Collection

Chiral-at-Metal Racemization Unraveled for $MX_2(a\text{-chel})_2$ by means of a Computational Analysis of $MoO_2(acnac)_2$

George Dhimba,[a] Alfred Muller,[a] and Koop Lammertsma*[a, b]

Octahedral chiral-at-metal complexes $MX_2(a\text{-chel})_2$ (a-chel = asymmetric chelate) can rearrange their ligands by four mechanisms known as the Bailar (B), Ray-Dutt (RD), Conte-Hippler (CH), and Dhimba-Muller-Lammertsma (DML) twists. Racemization involves their interconnections, which were computed for $MoO_2(acnac)_2$ (acnac = β-ketoiminate) using density functional theory at ωB97x-D with the 6-31G(d,p) and 6-311G(2d,p) basis sets and LANL2DZ for molybdenum. Racemizing the cis(NN) isomer, being the global energy minimum with trans oriented imine groups, is a three step process (DML-CH-DML) that requires 17.4 kcal/mol, while all three cis isomers (cis(NN), cis(NO), and cis(OO)) interconvert at ≤17.9 kcal/mol. The B and RD twists are energetically not competitive and neither are the trans isomers. The interconnection of all enantiomeric minima and transition structures is summarized in a graph that also visualizes valley ridge inflection points for two of the three CH twists. Geometrical features of the minima and twists are given. Lastly, the influence of N-substitution on the favored racemization pathway is evaluated. The present comprehensive study serves as a template for designing chiral-at-metal $MX_2(a\text{-chel})_2$ catalysts that may retain their chiral integrity.

Introduction

Chiral-at-metal catalysis differs from conventional asymmetric catalysis in that only the catalyst's metal center is stereogenic and none of its ligands.[1] The concept was conceived by Werner well over a century ago,[2] but chiral-at-metal catalysis is only recently gaining traction.[3] This belated advance is surprising given the importance of asymmetric catalysis in chemical conversions. Unnumerable catalysis studies have detailed the influence of a broad spectrum of chiral ligands (i.e., the "chiral pool") in search of reactions giving high enantiomeric or diastereomeric excess.[4] In sharp contrast, the number of studies using only the stereogenicity of the metal center have been few and far between. Undoubtedly, this disparity has its origin in the perceived ease of racemization when the metal center is five- or six-coordinate.[5] However, this is not necessarily the case as has been empirically demonstrated for, e.g., chiral ruthenium and iridium complexes.[1g,p]

Over half a century ago, the dynamics and topology of 5- and 6-coordination was addressed by Muetterties,[4f,6] but his seminal papers did not garner a following. This lackluster may be due to the near limitless number of racemization pathways for particularly 6-coordinate species. The possibilities are indeed perplexing for a hypothetical ML_6 complex with six different monodentate ligands that has potentially 30 different octahedral minima and 120 trigonal prismatic (transition) structures. However, introducing chelates results in a significant simplification and many chiral-at-metal catalysts have in fact two chelates. For 5-coordinate systems two appropriately sized bidentate ligands enable control of the Berry and Turnstile rotations so that chiral integrity can be enforced.[7] Expanding to 6-coordinate systems is the obvious next step.

Recently, we reported on the racemization of $MoO_2(acac)_2$ (acac = acetylacetonate)[8] and $MoO_2(nacnac)_2$ (nacnac = β-diketiminate),[9] which are 6-coordinate with two symmetrical bidentate ligands. Most surprisingly, we found two pathways that are more facile than the well-established Bailar (B)[10] and Ray-Dutt (RD)[11] twists and named them the Conte-Hippler (CH)[12] and Dhimba-Muller-Lammertsma (DML)[8,9] twists (Figure 1). This theoretical finding is in harmony with the topological analysis of Muetterties for $MX_2(chel)_2$ with symmetrical chelates. Interestingly, the CH twist is a valley ridge inflection that also connects to the trans isomer. The DML twist is the favored path for racemizing both $MoO_2(acac)_2$, concurring with an experimentally determined value,[12] and $MoO_2(nacnac)_2$.

Whereas these studies shed new light on feasible twists of 6-coordinate transition metal complexes, most of the used catalysts have asymmetric bidentate ligands (a-chel). The question then is how such $MX_2(a\text{-chel})_2$ systems behave? More specifically, how do the various twists contribute to racemization? Being able to answer this question is important for the design of chiral-at-metal catalysts that retain their chiral

[a] Dr. G. Dhimba, Prof. Dr. A. Muller, Prof. Dr. K. Lammertsma
Department of Chemical Sciences
University of Johannesburg
Auckland Park, Johannesburg, 2006 (South Africa)
E-mail: k.lammertsma@vu.nl

[b] Prof. Dr. K. Lammertsma
Department of Chemistry and Pharmaceutical Sciences, Faculty of Sciences
Vrije Universiteit Amsterdam
De Boelelaan 1108, 1081 HZ Amsterdam (The Netherlands)

Supporting information for this article is available on the WWW under https://doi.org/10.1002/chem.202302516

Special Collection Part of a Special Collection celebrating the 120th anniversary of the Royal Netherlands Chemical Society

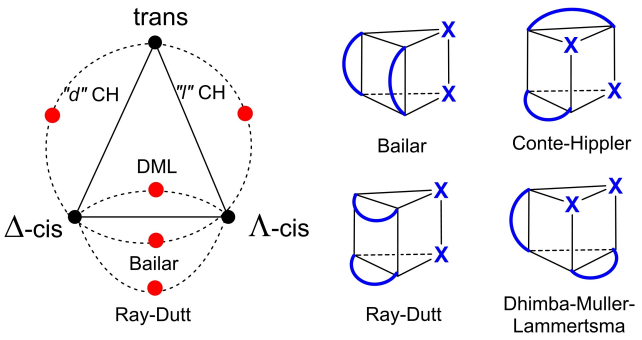

Figure 1. Topological representation of $MX_2(chel)_2$ with octahedral structures (black dots; energy minima) and connecting trigonal prismatic ones (red dots; transition structures) shown separately. The blue curved lines represent symmetrical chelates and the blue colored X monodentate ligands.

integrity. It requires a detailed understanding of all racemization and isomerization pathways as the a-chel ligands increase the complexity of racemization significantly. Here we present a full analysis (by means of B, RD, CH, and DML twists) for racemizing $MoO_2(acnac)_2$ (acnac = β-ketoiminate) which has two asymmetrical chelates that are each N- and O-coordinated to molybdenum. Ample $MoX_2(a\text{-}chel)_2$ complexes with acnac type ligands are known.[13] The present study extends those on $MoO_2(chel)_2$ (chel = acac, nacnac) and may serve as a general template for $MoX_2(a\text{-}chel)_2$.

Computational Details

The potential energy surface for all minima and transition structures was examined with Gaussian 16 ver. C01[14] using the hybrid meta-GGA functional ωB97X-D,[15] which incorporates empirical dispersion terms and long-range interactions.[16] The 6-31G(d) basis set was used for C, H, O, and N, and the LANL2DZ pseudopotential for Mo.[17] Frequency calculations were used to verify the nature of all stationary points with zero and one imaginary frequency for minima and transition structures, respectively. Intrinsic reaction coordinate (IRC) calculations confirmed all transition structures to be connected to minima along a given reaction path.[18] Single point calculations were performed with the larger 6-311 + G(2d,p) basis for selected structures.

Results and Discussion

The organization is that first all octahedral cis (and trans) minima are presented followed by the trigonal prismatic transition structures for each type of twist. Each of these sections will address what enantiomers (or isomers) are connected by a given twist and will highlight their characteristic geometrical features. From this we then identify the most likely racemization and rearrangement mechanism for cis isomers, analyze of the potential involvement of trans isomers, and provide a comprehensive picture to address all possible interconnections for chiral $MO_2(acnac)_2$. Lastly, the effect of N-substitution is briefly evaluated.

Minimum energy $MoO_2(acnac)_2$ structures

All minima adopt octahedral geometries. Those of the three enantiomeric pairs of cis-$MoO_2(acnac)_2$ are schematically depicted in Figure 2 and labeled (NN), (NO), or (OO) to reflect the trans orientation of the N and/or O chelate donor atoms. Figure 3 shows structures with the Mo=O ligands in trans positions. Trans(OO) has the O (and N) atoms of the two chelates on the same side of the MoO_2 unit and is chiral if the chelates are (slightly) twisted, which they are, while achiral trans(NO) has N and O atoms on either side.

The calculated $MoO_2(acnac)_2$ geometries for the Δ enantiomers of cis(NN), cis(NO), cis(OO), are shown in Figure 4 and those for trans(OO) and achiral trans(NO) in Figure 5. Their relative energies are listed in Table 1 and reveal cis(NN) to be the global minimum, favored over cis(NO) and cis(OO) by 3.9 and 8.0 kcal/mol, respectively. The trans(OO) isomer is 24.1 kcal/mol less stable and for trans(NO) the energy difference is even 54.5 kcal/mol, which compares to the cis-trans energy differences of both $MoO_2(acac)_2$ and $MoO_2(nacnac)_2$.[8,9]

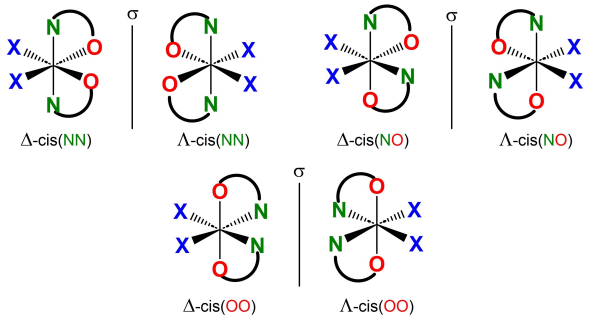

Figure 2. Schematic presentation of the octahedral structures of cis-$MoO_2(acnac)_2$ with the plane of symmetry (σ) separating the enantiomers. Blue colored X are the double bonded oxygens atoms.

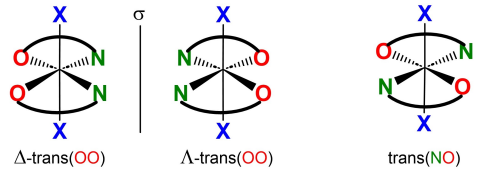

Figure 3. Schematic presentation of the enantiomeric and meso octahedral structures of trans-$MoO_2(acnac)_2$. Blue colored X are the trans double bonded oxygen atoms.

Table 1. Relative energies (in kcal/mol) of $MoO_2(acnac)_2$ minima.OO

Structures	ΔE	ν[a]
Δ/Λ-cis(NN)	0.0	16.5
Δ/Λ-cis(NO)	3.9	25.6
Δ/Λ-cis(OO)	8.0	24.0
Δ/Λ-trans(OO)	24.2	19.1
trans(NO)[b]	54.5	−53.4

[a] Smallest IR frequency in cm^{-1}. [b] Transition structure, optimized at 6-311 + + G(2d,p).

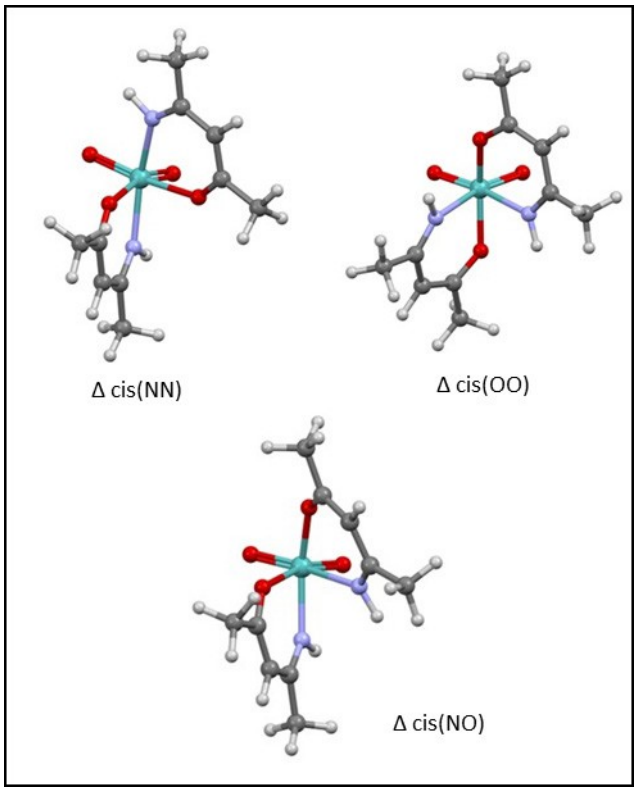

Figure 4. Calculated $MoO_2(acnac)_2$ structures for Δ-cis(NN), Δ-cis(NO), and Δ-cis(OO),.

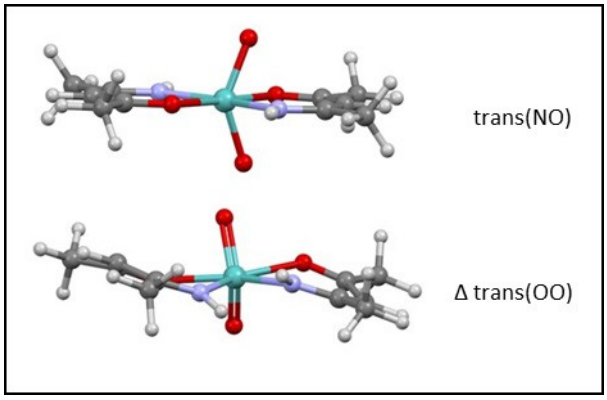

Figure 5. Calculated $MoO_2(acnac)_2$ structures for Δ-trans(OO) and trans(NO).

Geometries. The global cis(NN) minimum has Mo–N_{trans} and Mo–O_{cis} bonds lengths of 2.118 Å and 2.179 Å, respectively, with shorter Mo=O bonds of 1.702 Å. Its acnac planes have a dihedral angle of 72.4° and are 17.3° distorted from orthogonality with the MoO_2 fragment. The Mo–$N_{trans}/_{cis}$ and Mo–$O_{trans}/_{cis}$ bonds of the isomeric cis(NO) have lengths of respectively 2.117/2.340 Å and 1.995/2.185 Å, but its M=O bonds differ by only 0.002 Å. Compared to cis(NN), the dihedral angle formed by the planes of the two acnac ligands of cis(NO) is reduced by 17.7° while they have angles of 63.4 and 74.3° with the MoO_2 plane. The cis(OO) isomer has Mo–O_{trans} and Mo–N_{cis} bonds lengths of 2.010 Å and 2.320 Å, respectively. Its acac ligand planes have a 7.2 ° larger dihedral angle than in cis(NN) and deviate only slightly (by $<5°$) from orthogonality with the MoO_2 plane.

Chiral trans(OO) has its ligand N–H atoms on the same side of the MoO_2 unit but tilted by 15° from ligand planarity in opposite directions to minimize H···H repulsion. Trans(NO) has C_s symmetry at 6-311++G(2d,p) with both acnac ligands oriented in the same plane with the dioxo ligands of the orthogonal MoO_2 plane bend by 140 ° towards one of the acnac ligands. It resembles the C_{2v} symmetrical trans-$MoO_2(acac)_2$.[8]

Bailar and Ray-Dutt twists.

Three Bailar (B) and three Ray-Dutt (RD) transition structures were located. They are schematically depicted in Figure 6. B-2 and m-B-2 represent an enantiomeric pair as do RD-2 and m-RD-2 (m stands for mirror).

Achiral B-1 and RD-1 are the two twists that racemize Δ- and Λ-cis(NO). Chiral Λ-B-2 and Λ-RD-2 are the two transition structures that connect Λ-cis(NN) with Δ-cis(OO), while the corresponding mirror images Δ-B-2 and Δ-RD-2 connect, of course, Δ-cis(NN) with Λ-cis(OO). The signature of these twists are given in Equations (1)–(3) and were confirmed by their IRC trajectories (see Supporting Information).

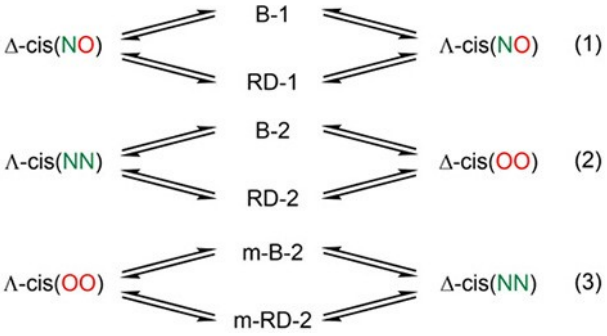

Figure 7 shows the transition structures. Their relative energies, given in Table 2, make clear that the B and RD twists have both significant barriers of more than 24 kcal/mol. Equations (1)–(3) emphasize that these twists are inadequate to

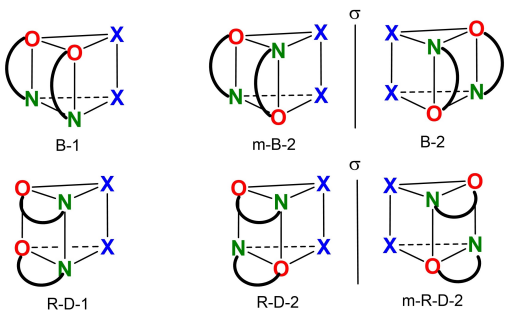

Figure 6. Schematic presentation of the three Bailar and three Ray-Dutt transition structures for cis-$MoO_2(acnac)_2$. Blue colored X are the double bonded oxygen atoms.

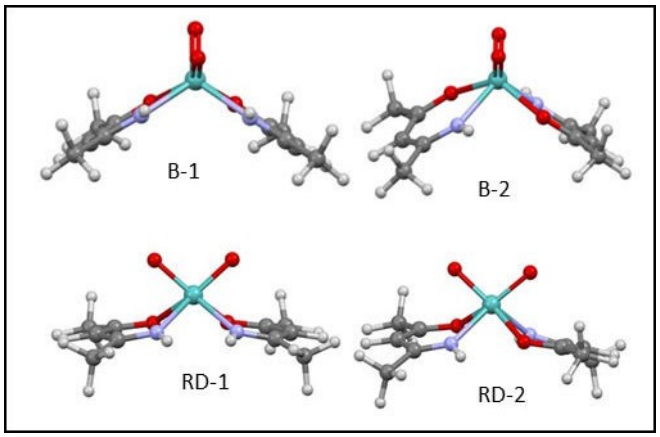

Figure 7. Calculated $MoO_2(acnac)_2$ transition structures for the Bailar twists (B-1 and B-2), the Ray-Dutt twists (RD-1 and RD-2).

Table 2. Energies (in kcal/mol) of Bailar and Ray-Dutt $MoO_2(acnac)_2$ transition structures relative to cis(NN).

Structures	ΔE	ν[a]
B-1	24.2	67
Δ,Λ-B-2	25.0	95
RD-1	34.0	107
Δ,Λ-RD-2	26.4	94

[a] Single imaginary frequency in cm^{-1}.

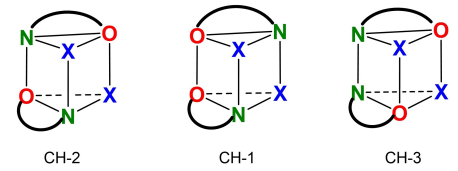

Figure 8. Schematic presentation of the three Conte-Hippler transition structures for cis-$MoO_2(acnac)_2$. Blue colored X are the double bonded oxygen atoms.

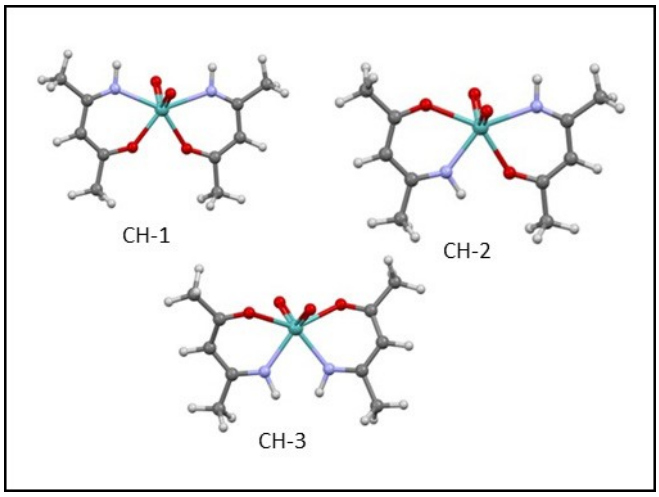

Figure 9. Calculated $MoO_2(acnac)_2$ transition structures for the Conte-Hippler twists (CH-1, CH-2, and CH-3).

Table 3. Energies (in kcal/mol) of Conte-Hippler and Dhimba-Muller-Lammertsma $MoO_2(acnac)_2$ transition structures relative to cis(NN).

Structures	ΔE	ν[a]
CH-2	17.4	30
CH-1	21.6	41
CH-3	24.7	51
DML-1	14.8	65
DML-2	17.9	79

[a] Single imaginary frequency in cm^{-1}.

explain full racemization of $MoO_2(acnac)_2$.There must be additional pathways.

Geometries. The B-1 transition structure (C_s sym.) has its MoO_2 unit bisecting the two ligand planes (∠ = 115.9°; *d*MoO = 2.191 Å, *d*MoN = 2.149 Å,) with an angle of 122.0°. For chiral B-2 (C_2 sym.) MoO_2 has a similar bisecting angle of 121.8° with the ligand planes (∠ = 111.2°; *d*MoO = 2.150 Å, *d*MoN = 2.180 Å). The MoO_2 unit of the RD-1 structure (C_s sym.) is rotated by 90° compared to B-1 and bisects (∠ = 91.2°) the virtually parallel ligand planes (∠ = 13.8°; *d*MoO = 2.119 Å, *d*MoN = 2.199 Å) with the molybdenum atom lying 1.046 Å above them. Chiral RD-2 (C_2 sym.) has similar characteristic with an angle of 19.5° between the ligand planes (*d*MoO = 2.149 Å, *d*MoN = 2.159 Å).

Conte-Hippler twists

Earlier we established the presence of a Conte-Hippler (CH) twist for $MoO_2(acac)_2$ with a ca. 8 kcal/mol lower energy barrier than both the B and RD twists.[8] For $MoO_2(nacnac)_2$ the corresponding CH–B energy difference is nihil and amounts to 11 kcal/mol for CH-RD.[9] For the present $MoO_2(acnac)_2$ we found, in fact, three CH twists, shown schematically in Figure 8, one for each enantiomer pair, as shown in Equations (4)–(6). The geometries of the transition structures are shown in Figure 9, their relative energies are listed in Table 3, and their IRC trajectories are given in the Supporting Information. The CH-1 and CH-2 structures are achiral with C_{2v} or C_s symmetries, respectively. The potential energy surface surrounding non-planar, chiral CH-3, is actually more complex than suggested in Equation (6) and this will be addressed in a subsequent section.

$$\Delta\text{-cis(NO)} \rightleftharpoons \text{CH-2} \rightleftharpoons \Lambda\text{-cis(NO)} \quad (4)$$

$$\Delta\text{-cis(NN)} \rightleftharpoons \text{CH-1} \rightleftharpoons \Lambda\text{-cis(NN)} \quad (5)$$

$$\Delta\text{-cis(OO)} \rightleftharpoons \text{CH-3} \rightleftharpoons \Lambda\text{-cis(OO)} \quad (6)$$

Geometries. The lowest energy CH-2 transition structure (C_s sym.) has its acnac ligands (*d*MoO = 2.084/2.258 Å and *d*MoN = 2.230/2.110 Å) lying in a single plane with the two 1.704 Å M=O bonds of the orthogonal MoO_2 unit (∠OMoO = 116.9°) directed equally above and below. C_{2v} symmetrical CH-1 is similar to CH-

2 with *d*MoO and *d*MoN ligand bond lengths of 2.048 Å and 2.265 Å, respectively. In chiral CH-3 (C_2 sym.) the angle between the two ligand planes (*d*MoO = 2.200 Å, *d*MoN = 2.139 Å) amounts to 38.9°; the angle of each ligand plane with the MoO_2 amounts to 123°.

Dhimba-Muller-Lammertsma twists

There are two enantiomeric sets of DML transition structures. These are schematically depicted in Figure 10. DML-2 connects Δ-cis(NO) with Λ-cis(OO) and its mirror image (m-DML-2) connects the corresponding enantiomers Λ-cis(NO) and Δ-cis(OO). The other twist, DML-1, connects Λ-cis(NO) with Δ-cis(NN) and their enantiomers are connected by m-DML-1. These relationships are reflected in Equations (7)–(10). The signature of these twists were confirmed by their IRC trajectories (see Supporting Information). The relative energies are given in Table 3 and their geometries are shown in Figure 11.

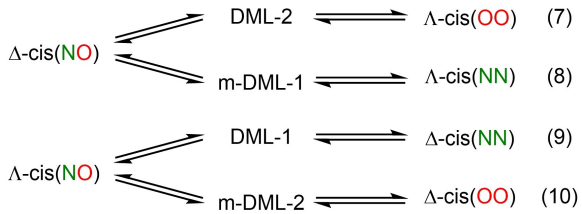

The DML-1 twist (ΔE = 14.8 kcal/mol) is the most favorable transition structure of all and mimics both $MoO_2(acac)_2$ and $MoO_2(nacnac)_2$.[8,9] The next best is DML-2 with is nearly isoenergetic with the CH-2 twist (ΔΔE = 0.5 kcal/mol).

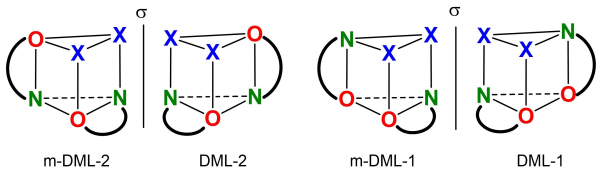

Figure 10. Schematic presentation of the two enantiomer sets of Dhimba-Lammertsma-Muller transition structures for cis-$MoO_2(acnac)_2$. Blue colored X are the double bonded oxygen atoms.

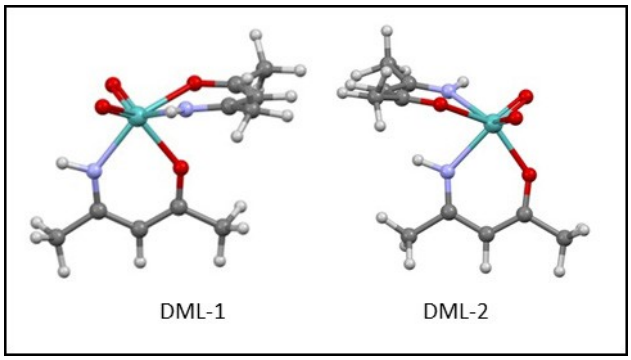

Figure 11. Calculated $MoO_2(acnac)_2$ transition structures for the Conte-Hippler twists (CH-1, CH-2, and CH-3), and the Dhimba-Muller-Lammertsma twists (DML-1 and DML-2).

The two acnac ligand planes of DML-1 (*d*MoO = 2.107/2.186 Å and *d*MoN = 2.142/2.184 Å) are essentially orthogonal (∠ = 85.9°). The MoO_2 unit's oxygen atoms lie in one of the acnac planes that has a shortest distance to the molybdenum atom of 0.65 Å and an angle of 35.8° with the MoO_2 unit plane. The features of the DML-2 structure are pretty much similar to those of DML-1 with as distinguishing feature a full 180° rotation of one of the acnac ligands.

Racemizing $MoO_2(acnac)_2$

With three cis and two trans $MoO_2(acnac)_2$ minima and nine transition structures, connecting the various enantiomers may seem complex. A topological analysis might help to digest the racemization pathways, but it would not give the distinguishing details that are embedded in an evaluation of the potential energy surface. To get such insight we start by addressing how the enantiomeric minima are linked and cross-linked.

The favored cis(NN) isomer has only one single-step racemization pathway, being the CH-1 twist (ΔE = 21.6 kcal/mol). Likewise, the much less stable cis(OO) isomer (ΔE = 8.0 kcal/mol) also has only one direct path for racemization, namely the CH-3 twist (ΔE = 24.7 kcal/mol). Instead, the cis(NO) isomer (ΔE = 3.9 kcal/mol) can racemize by three different single-step processes of which the CH-2 twist (ΔE = 17.4 kcal/mol) is favored by far over the B and RD twists. Hence, to establish whether cis(NN) has a lower racemization barrier than the noted 21.6 kcal/mol (i.e., CH-1), the 'cross-links' with its cis(NO) and cis(OO) isomers need to be considered, particularly because cis(NO) has a low racemization barrier (i.e., CH-2; ΔΔE = 13.5 kcal/mol).

Since the rearrangement of the isomers by means of both the B and RD twists are energetically not competitive, the focus shifts to the much more favorable DML twist of which there are two. They provide an opening. Thus, cis(NN) isomer can rearrange to the cis(NO) isomer by means of the DML-1 twist that has a barrier of only 14.8 kcal/mol. This means that the lowest energy pathway to racemize cis(NN) is a three-step process (Figure 12). The first step is a DML-1 rearrangement of an enantiomer of cis(NN) to cis(NO), upon which racemization occurs by means of the CH-2 twist, followed by another DML-1 rearrangement to give the other enantiomer of cis(NN).

The other low-energy rearrangement, the DML-2 twist of 17.9 kcal/mol, interconverts the less stable cis(OO) and cis(NO) isomers and is therefore not an alternative racemization pathway. Instead, it merely illustrates enantioselective isomerization of the three cis-$MoO_2(acnac)_2$ isomers (dashed red line in Figure 10). This means that all isomers rearrange and racemize within 17.9 kcal/mol, only 0.5 kcal/mol above the racemization barrier.

Research Article
doi.org/10.1002/chem.202302516
Chemistry Europe
European Chemical Societies Publishing

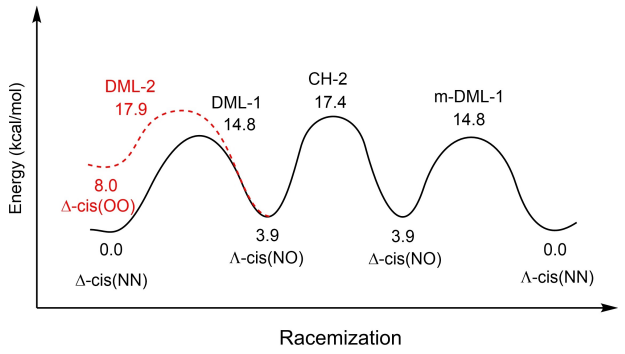

Figure 12. Energy profile for the preferred racemization pathway (in black) for the global minimum cis(NN) of cis-MoO2(acnac)$_2$. The dashed red line shows the isomerization pathway for Λ-cis(NO) and Δ-cis(OO).

Trans-$MoO_2(acnac)_2$

Trans(NO) and trans(OO) must also be evaluated not only for completeness but also for their relationship with the CH twists. After all, these are valley ridge inflections for cis-$MoO_2(acac)_2$ and connect the two enantiomers with the high-energy trans isomer ($\Delta E = 50.9$ kcal/mol);[8] this is likewise the case for $MoO_2(nacnac)_2$ ($\Delta E(trans) = 54.3$ kcal/mol).[9] The same behavior is found for trans(NO) ($\Delta E = 54.5$ kcal/mol). Thus, whereas CH-2 is the favored twist for racemizing cis(NO), it is also connected to high-energy trans(NO) and is thus also a valley-ridge inflection point.

CH-3 is the chiral transition structure (C_2 sym.) for racemizing cis(OO) [Equation (6)] by either a left- or right-handed motion. The Δ- and Λ-trans(OO) minima are only 0.5 kcal/mol more stable than the enantiomeric CH-3 transition structures to which they are connected. Hence Δ- and Λ-CH-3 are both valley-ridge inflection points. The potential energy surface in this region is rather flat ($\Delta E \approx 25$ kcal/mol), requiring < 0.5 kcal/mol to convert Δ-trans(OO) into Δ-cis(OO) (see Figure S3 in the Supporting Information).

Diagram of the dynamics of $MoO_2(acnac)_2$

The entire ensemble of enantiomeric minima and transition structures of cis-$MoO_2(acnac)_2$ (and the trans forms) together with all the feasible twists can be captured in the single graph shown in Figure 13. In whatever way we may want to picture the graph, it remains complex and begs for simplification. A bold simplification is to remove from the graph all the Bailar and Ray-Dutt twists. Whereas these twists are well established, be it primarily for trichelate complexes, such a simplification is justified because they are energetically not competitive with the CH and DML twists as explained above and as shown earlier for the related cis-$MoO_2(acac)$[8] and cis-$MoO_2(nacnac)_2$.[9]

The resulting simplified graph in which all minima (cis(NN), cis(NO), cis(OO), trans(NO), and trans(OO)) are connected by only CH and DML twists is given in Figure 14, which also gives the relative energies.

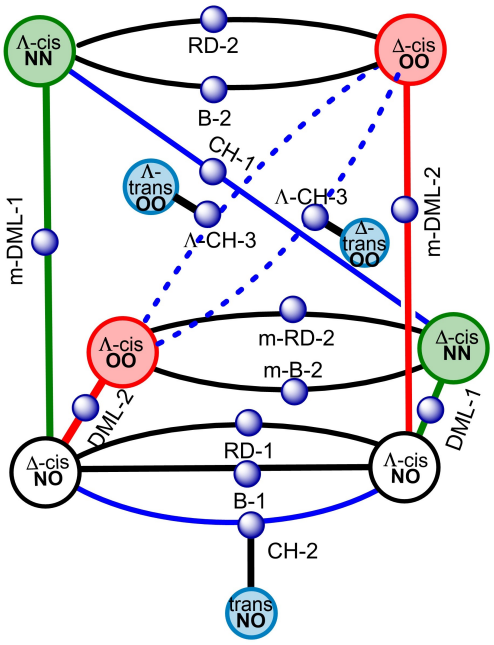

Figure 13. Diagram of $MoO_2(acnac)_2$. Minima are encircled. The smaller shaded blue balls are transition structures, labeled with the twist they represent. Cis(NN), cis(NO), and cis(OO) are shown in green, white, and red circles, respectively, and trans(NO) and Δ- and Λ-trans(OO) in smaller blue circles.

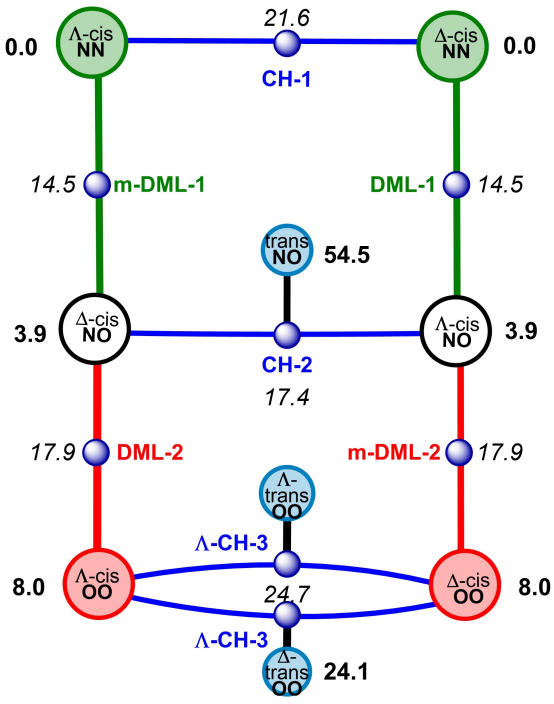

Figure 14. Simplified diagram of $MoO_2(acnac)_2$ with all minima connected by only CH and DML twists. Minima for cis(NN), cis(NO), and cis(OO) are shown in green, white, and red circles, respectively, and in blue for trans(NO) and trans(OO). The smaller shaded blue balls are the CH and DML transition structures. The green lines are for the DML-1 twists, the red lines those for DML-2, the blue ones for all three CH twists, and the black ones for the connection of the trans structures with the CH-2 and CH-3 structures. Relative energies (in kcal/mol) of minima are shown in boldface and those for transition structures in italics.

The graph gives a more comprehensive picture than the conventional potential energy surface show in Figure 12. It illustrates nicely that the three-step racemization pathway for the global minimum cis(NN) by means of DML-1, CH-2, and m-DML-1) is favored over the single-step CH-1 twist by a significant 4.2 kcal/mol. For completeness, it must be stressed that whereas the B nor RD twists are prominent for $M(chel)_3$ complexes, their role is insignificant in the racemization of $MoO_2(acnac)_2$. First, such twists do not exist for the enantiomeric cis(NN). Second, the B-1 and RD-1 twists for racemizing cis(NO) are an impressive 6.8 and 16.6 kcal/mol, respectively, more demanding than the rate-determining CH-2 twist. Said differently, the lowest energy pathway for the three isomeric structures on the left-hand side of the graph to their enantiomers on the right-hand side of the graph is by way of the CH-2 twist.

Effect of N-substitution

How would N-substitution of the ligands effect the twist barriers? Earlier we have shown that replacing acac ligands for nacnac ligands reduces the barriers, while bulky N-substituents raise them significantly.[9] Therefore, the effect of substituting the N-centers of the acnac ligands is expected to be limited. This is exactly what is found. We chose the sizeable N-phenyl group and examined the influence on the relative energies of the cis-$MoO_2(acnac)^{Ph2}$ minima and the DML and CH-2 twist barriers. The relative energies (6-31G(d) with LanL2DZ for Mo) are listed in Table 4. All structures are significantly influenced by the two phenyl substituents (see Supporting Information) but the effect on the potential energy surface is modest.

There are three important observations. First, the relative energy differences of the minima reduce to the extent that the cis(NO) and cis(OO) isomers become isoenergetic. Second, and relevant from a practical point of view, the DML-1 and DML-2 barriers increase by 3.9 to 4.5 kcal/mol to respectively 18.9 and 22.4 kcal/mol. Third, CH-2 barrier increases likewise by 5.3 to 22.8 kcal/mol. Consequently, rapid racemization will still occur at room temperature, but our preliminary excursion suggests an impact of steric factors on the twist barriers.

Table 4. Energies (in kcal/mol) of $MoO_2(acnac)_2^{Ph2}$ minima and DML transition structures.

Structures	ΔE	ν[a]
Δ/Λ-cis(NO)	0.0	35
Δ/Λ-cis(OO)	0.1	27
Δ/Λ-cis(NN)	3.8	21
DML-1	18.9	−54
DML-2	22.4	−72
CH-2	22.8	2

[a] Smallest IR frequency and single DML imaginary frequencies in cm^{-1}.

Mo-ligand bond cleavage

Of course, there is always the possibility that a chelate partly detaches to give a pentacoordinate complex that subsequently reforms the hexacoordinate complex. Such a pathway may also cause racemization of a chiral-at-metal complex, but it is clearly distinct from the discussed non-dissociating twists. For completeness, we evaluated acnac ligand dissociation for the cis(NN) isomer of the parent $MoO_2(acnac)_2$. Its Mo–O/N bond cleavage results in Mo-pentacoordination but requires 29.3 kcal/mol. Moreover, the resulting complexes are 20 kcal/mol less stable than the global cis(NN) minimum. The details are presented in Figure S4 in the Supporting Information. Consequently, this route seems to be less viable for racemizing $MoO_2(acnac)_2$ than the non-dissociating twist discussed in this paper.

Conclusions

The underlying mechanisms for non-dissociative racemization of chiral-at-metal complexes $MX_2(a\text{-}chel)_2$ (a-chel = asymmetric chelate) was computationally examined for $MoO_2(acnac)_2$ using the ωB97x-D functional and the 6-31G(d,p) basis set for C, H, O, and N and LANL2DZ for Mo. The three octahedral cis complexes are subject to Bailar (B), Ray-Dutt (RD), Conte-Hippler (CH), and Dhimba-Muller-Lammertsma (DML) twists. Racemizing the cis(NN) global minimum is a three step process (DML-CH-DML) that requires 17.4 kcal/mol, while all cis isomers (cis(NN), cis(NO), and cis(OO)) interconvert at ≤ 17.9 kcal/mol. Whereas B and RD twists are prevalent in trichelate complexes, they are energetically not competitive for dichelate complexes and neither are the trans isomers. The interconnection of all enantiomeric minima and transition structures can be summarized in a comprehensive graph (Figure 13) that also visualizes valley ridge inflection points for two of the three CH twists. Racemization (and isomerization) can also be summarized in a simplified graph (Figure 14) with only CH and DML twists. Whereas N-substitution influences the relative energies of the three cis isomers and effects the twist barriers, the effects are modest. The present comprehensive study, the first of its kind, can serve as a template for $MX_2(a\text{-}chel)_2$ and assist in the design of chiral-at-metal catalysts. The challenge is to inhibit the pathways for non-dissociative racemization in order for the catalyst to retain its chiral integrity. The present study provides the insights to enable this.

Acknowledgements

We gratefully acknowledge the support of the National Research Foundation (Grant 120842) and the Centre for High Performance Computing (CHPC) of South Africa.

Conflict of Interests

The authors declare no conflict of interest.

Data Availability Statement

The data that support the findings of this study are available in the supplementary material of this article.

Keywords: coordination modes · density functional calculations · homogeneous catalysis · molybdenum · N,O-ligands

[1] a) M. Chavarot, S. Ménage, O. Hamelin, F. Charnay, J. Pécaut, M. Fontecave, *Inorg. Chem.* **2003**, *42*, 4810–4816; b) O. Hamelin, M. Rimboud, J. Pécaut, M. Fontecave, *Inorg. Chem.* **2007**, *46*, 5354–5360; c) C. Ganzmann, J. A. Gladysz, *Chem. Eur. J.* **2008**, *14*, 5397–5400; d) H. Huo, C. Fu, K. Harms, E. Meggers, *J. Am. Chem. Soc.* **2014**, *136*, 2990–2993; e) C. Wang, L.-A. Chen, H. Huo, X. Shen, K. Harms, L. Gong, E. Meggers, *Chem. Sci.* **2015**, *6*, 1094–1100; f) Y. Zheng, Y. Tan, K. Harms, M. Marsch, R. Riedel, L. Zhang, E. Meggers, *J. Am. Chem. Soc.* **2017**, *139*, 4322–4325; g) T. Cruchter, M. G. Medvedev, X. Shen, T. Mietke, K. Harms, M. Marsch, E. Meggers, *ACS Catal.* **2017**, *7*, 5151–5162; h) J. Ma, X. Ding, Y. Hu, Y. Huang, L. Gong, E. Meggers, *Nat. Commun.* **2014**, *5*, 4531; i) H. Huo, X. Shen, C. Wang, L. Zhang, P. Röse, L.-A. Chen, K. Harms, M. Marsch, G. Hilt, E. Meggers, *Natur.* **2014**, *515*, 100–103; j) Y. Tan, W. Yuan, L. Gong, E. Meggers, *Angew. Chem.* **2015**, *127*, 13237–13240; k) Y. Hu, Z. Zhou, L. Gong, E. Meggers, *Org. Chem. Front.* **2015**, *2*, 968–972; l) H. Huo, K. Harms, E. Meggers, *J. Am. Chem. Soc.* **2016**, *138*, 6936–6939; m) V. A. Larionov, T. Cruchter, T. Mietke, E. Meggers, *Organometallics* **2017**, *36*, 1457–1460; n) H. Lin, Z. Zhou, J. Cai, B. Han, L. Gong, E. Meggers, *J. Org. Chem.* **2017**, *82*, 6457–6467; o) T. Mietke, T. Cruchter, V. A. Larionov, T. Faber, K. Harms, E. Meggers, *Adv. Synth. Catal.* **2018**, *360*, 2093–2100; p) C.-X. Ye, E. Meggers, *Acc. Chem. Res.* **2023**, *56*, 1128–1141.

[2] a) A. Werner, *Ber. Dtsch. Chem. Ges.* **1914**, *47*, 2171–2182; b) A. Werner, *Ber. Dtsch. Chem. Ges.* **1911**, *44*, 2445–2455; c) A. Werner, *Ber. Dtsch. Chem. Ges.* **1911**, *44*, 3272–3278; d) A. Werner, *Ber. Dtsch. Chem. Ges.* **1911**, *44*, 3279–3284.

[3] a) H. B. Kagan, *Asymm. Synth.* **1985**, *5*; b) A. Pfaltz, W. J. Drury III, *PNAS* **2004**, *101*, 5723–5726; c) G. Yang, W. Zhang, *Chem. Soc. Rev.* **2018**, *47*, 1783–1810; d) M. Glos, O. Reiser, *Org. Lett.* **2000**, *2*, 2045–2048; e) O. Chuzel, O. Riant, *Top. Organomet. Chem.* **2005**, *15*, 59–92; f) S. P. Flanagan, P. J. Guiry, *J. Organomet. Chem.* **2006**, *691*, 2125–2154; g) M. McCarthy, P. J. Guiry, *Tetrahedron* **2001**, *57*, 3809–3844; h) J. F. Teichert, B. L. Feringa, *Angew. Chem. Int. Ed.* **2010**, *49*, 2486–2528; i) Y. Huang, T. Hayashi, *Chem. Rev.* **2022**, *122*, 14346–14404.

[4] a) S. Alvarez, *Chem. Rev.* **2015**, *115*, 13447–13483; b) W. Zou, Y. Tao, E. Kraka, *J. Chem. Theory Comput.* **2020**, *16*, 3162–3193; c) P. Gillespie, P. Hoffman, H. Klusacek, D. Marquarding, S. Pfohl, F. Ramirez, E. Tsolis, I. Ugi, *Angew. Chem. Int. Ed.* **1971**, *10*, 687–715; d) R. S. Berry, *J. Chem. Phys.* **1960**, *32*, 933–938; e) P. Meakin, E. L. Muetterties, J. P. Jesson, *J. Am. Chem. Soc.* **1972**, *94*, 5271–5285; f) E. L. Muetterties, *J. Am. Chem. Soc.* **1968**, *90*, 5097–5102.

[5] a) Z. Zhou, S. Chen, Y. Hong, E. Winterling, Y. Tan, M. Hemming, K. Harms, K. N. Houk, E. Meggers, *J. Am. Chem. Soc.* **2019**, *141*, 19048–19057; b) J. Ma, J. Lin, L. Zhao, K. Harms, M. Marsch, X. Xie, E. Meggers, *Angew. Chem. Int. Ed.* **2018**, *57*, 11193–11197.

[6] a) E. L. Muetterties, *Inorg. Chem.* **1967**, *6*, 635–638; b) E. L. Muetterties, *J. Am. Chem. Soc.* **1969**, *91*, 1636–1643; c) E. L. Muetterties, *J. Am. Chem. Soc.* **1969**, *91*, 4115–4122.

[7] L. J. P. van der Boon, L. van Gelderen, T. R. de Groot, M. Lutz, J. C. Slootweg, A. W. Ehlers, K. Lammertsma, *Inorg. Chem.* **2018**, *57*, 12697–12708.

[8] G. Dhimba, A. Muller, K. Lammertsma, *Inorg. Chem.* **2022**, *61*, 14918–14923.

[9] G. Dhimba, A. Muller, K. Lammertsma, *Eur. J. Inorg. Chem.* e202300256.

[10] J. C. Bailar Jr, *J. Inorg. Nucl. Chem.* **1958**, *8*, 165–175.

[11] P. Ray, N. Dutt, *J. Indian Chem. Soc.* **1943**, *20*, 81–92.

[12] M. Conte, M. Hippler, *J. Phys. Chem. A* **2016**, *120*, 6677–6687.

[13] a) J. L. Brown, C. C. Mokhtarzadeh, J. M. Lever, G. Wu, T. W. Hayton, *Inorg. Chem.* **2011**, *50*, 5105–5112; b) H. Na, P. N. Lai, L. M. Cañada, T. S. Teets, *Organometallics* **2018**, *37*, 3269–3277; c) N. C. Ou, X. Su, D. C. Bock, L. McElwee-White, *Coord. Chem. Rev.* **2020**, *421*, 213459; d) X. Su, P. Panariti, K. A. Abboud, L. McElwee-White, *Polyhedron* **2019**, *169*, 219–227.

[14] Gaussian 16, Revision C.01, G. W. Trucks, H. B. Schlegel, G. E. Scuseria, M. A. Robb, J. R. Cheeseman, G. Scalmani, V. Barone, G. A. Petersson, H. Nakatsuji, X. Li, M. Caricato, A. V. Marenich, J. Bloino, B. G. Janesko, R. Gomperts, B. Mennucci, H. P. Hratchian, J. V. Ortiz, A. F. Izmaylov, J. L. Sonnenberg, Williams, F. Ding, F. Lipparini, F. Egidi, J. Goings, B. Peng, A. Petrone, T. Henderson, D. Ranasinghe, V. G. Zakrzewski, J. Gao, N. Rega, G. Zheng, W. Liang, M. Hada, M. Ehara, K. Toyota, R. Fukuda, J. Hasegawa, M. Ishida, T. Nakajima, Y. Honda, O. Kitao, H. Nakai, T. Vreven, K. Throssell, J. A. Montgomery Jr., J. E. Peralta, F. Ogliaro, M. J. Bearpark, J. J. Heyd, E. N. Brothers, K. N. Kudin, V. N. Staroverov, T. A. Keith, R. Kobayashi, J. Normand, K. Raghavachari, A. P. Rendell, J. C. Burant, S. S. Iyengar, J. Tomasi, M. Cossi, J. M. Millam, M. Klene, C. Adamo, R. Cammi, J. W. Ochterski, R. L. Martin, K. Morokuma, O. Farkas, J. B. Foresman, D. J. Fox, *Gaussian Inc.*, Wallingford, CT, **2016**.

[15] J.-D. Chai, M. Head-Gordon, *Phys. Chem. Chem. Phys.* **2008**, *10*, 6615–6620.

[16] Y. Minenkov, Å. Singstad, G. Occhipinti, V. R. Jensen, *Dalton Trans.* **2012**, *41*, 5526–5541.

[17] a) M. Couty, M. B. Hall, *J. Comput. Chem.* **1996**, *17*, 1359–1370; b) Y. Yang, M. N. Weaver, K. M. Merz, *J. Phys. Chem. A* **2009**, *113*, 9843–9851; c) P. J. Hay, W. R. Wadt, *J. Chem. Phys.* **1985**, *82*, 270–283.

[18] a) C. Gonzalez, H. B. Schlegel, *J. Chem. Phys.* **1989**, *90*, 2154–2161; b) C. Gonzalez, H. B. Schlegel, *J. Phys. Chem.* **1990**, *94*, 5523–5527.

Manuscript received: August 2, 2023
Accepted manuscript online: September 20, 2023
Version of record online: ■■, ■■

RESEARCH ARTICLE

Racemization mechanisms of chiral-at-metal $MX_2(a\text{-chel})_2$ complexes were unraveled using $MoO_2(acnac)_2$ as a model. The cis(NN) isomer is the global energy minimum and racemizes via a three-step mechanism DML→ CH→DML, which serves as prototype for racemizing $MX_2(a\text{-chel})_2$.

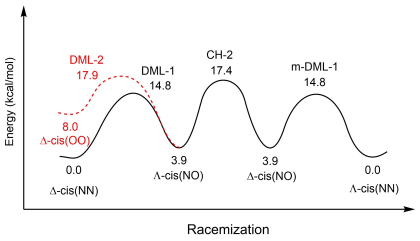

*Dr. G. Dhimba, Prof. Dr. A. Muller, Prof. Dr. K. Lammertsma**

1 – 9

Chiral-at-Metal Racemization Unraveled for $MX_2(a\text{-chel})_2$ by means of a Computational Analysis of $MoO_2(acnac)_2$